Iranian Journal of Geophysics, Vol 18 No 3, 2024, Page 1 – 21 (Research Article)
DOI: 10.30499/IJG.2023.389984.1508

Determination of two-dimensional shear-wave velocity profiles using single-station and array measurements of ambient noises in Hakimiyeh valley, Tehran, Iran

Mojtaba Siavashpour[1], Ebrahim Haghshenas[2] and Mohsen Fazlavi[3*]

[1] *Ph.D., International Institute of Earthquake Engineering and Seismology (IIEES), Tehran, Iran*
[2] *Associate Professor, Department of Geotechnical Engineering, International Institute of Earthquake Engineering and Seismology (IIEES), Tehran, Iran*
[3] *Assistant Professor, Department of Civil Engineering and Architecture, Faculty of Enghelab-e Eslami, Technical and Vocational University (TVU), Tehran, Iran*

(Received: 18 March 2023, Accepted: 03 September 2023)

Abstract

The shear-wave velocity (Vs) of soils has been acknowledged among the most critical factors affecting the nature of seismic surface motions, known as seismic site effects, in the course of probable earthquakes. Together with the one-dimensional (1D) Vs profiles of soils, the lateral heterogeneity of velocity contrasts may strongly impact seismic ground motions within the surface. Such conditions seem to occur in the city of Tehran, Iran, mainly in the eastern part, Hakimiyeh Valley, wherein alluvial deposits have been settled between the Alborz and Sepayeh (the Anti-Alborz) mountain ranges. In this resepct, the significant differences observed between previous analytical and empirical studies doubles the necessity of estimating real bedrock depth and Vs structure in this area. Given that the improper analysis of seismic site effects, using unrealistic dynamic characteristics, gives rise to the low-accuracy prediction of seismic hazards as well as significant human and financial losses; this study is an attempt to extract the two-dimensional (2D) Vs structure of the subsurface layers in the form of two north-south and east-west profiles, through the single-station and array measurements of ambient noises (viz., microtremors), as the first deep alluvial models in this area. For this purpose, the ambient noises are recorded with reference to 4 and 11 array and single-station measurements, respectively. A circular layout, comprised of two concentric circles, is further considered for the array measurements with 11 three-component narrow-band seismometers, Lennartz LE-3D/20S, within each array. The recorded array seismograms are then analyzed via the spatial autocorrelation (SPAC) method and the frequency-wavenumber (F-K) analysis, and all seismograms recorded in this line are subsequently evaluated by the time-frequency analysis (TFA) of ellipticity in the Geopsy software. Afterward, the results are utilized as the objective functions (OFs) in the inversion operation for calculating the Vs profiles at the selected stations. The neighborhood algorithm is further applied for the inversion of the OFs and the extraction of the Vs profiles. The study results as it comes to the extraction of the 2D profiles and the recognition of the Vs structure in this area, along with the velocity of 2200 m/s, correspond to the seismic bedrock located in the deepest part of the sedimentary basin, 800 m. Moreover, the underground topographies, such as faults, can be identified in the Vs profiles by means ofusing the ambient noises. As a final point, the profiles indicate that the variations in the Vs and dynamic properties of the soil are significant in this area, as one with a complicated subsurface structure. The dominant frequencies of the sediments in Hakimiyeh Valley, reported in previous analytical research, are also significantly different from that those extracted in this empirical study. As an illustration, no sharp and clear peaks can be spotted in the analytical amplification functions in Hakimiyeh Valley, while there are distinct peaks below 2 Hz at most stations in the present study. Furthermore, the study results are in good agreement with the geology of this area, and pave the ground for analytical site effect studies in the future.

Keywords: Tehran Alluvium, shear-wave velocity, ambient noise, ellipticity, site effects

[*]Corresponding author: mfazlavi@tvu.ac.ir

1 Introduction

The properties of seismic waves significantly change while passing through alluvial layers near the surface, far away from the focal points of earthquakes, known as seismic site effects. Such variations appear as the frequency-depended amplification or de-amplification of motions as well as changes in motion duration. To give an example, the 1985 Mexico City earthquake in Mexico with a moment magnitude of 8.1 caused moderate damage in the areas around its epicenter (namely, the Pacific Ocean beaches), but seriously destroyed the great Mexico City, 350 km far from the focal point due to the existence of soft soil underneath the city, which enormously amplified long-period seismic waves (Foutch et al., 1989).

The accurate examination of seismic site effects, such as the Mexico City case, has been thus accredited as one of the main goals of geotechnical earthquake engineering, which demands sufficient knowledge and awareness of geological conditions and shear-wave velocity (Vs) structures. This is of utmost importance in Tehran, as Iran's political capital and one of the world's largest metropolitan areas. Continuous population growth and the increasing trend in the construction of high-rise buildings in this megacity, built over a very thick alluvial deposit nearby numerous active faults, are among the critical factors that excessively multiply seismic damages and risks in this city.

A limited number of comprehensive studies have already been implemented on site effects in Tehran, including those by Jafari (2001) and JICA (2000), fulfilled by the Japan International Cooperation Agency and Center for Earthquake and Environmental Studies of Tehran (CEST). These two studies have so far provided seismic hazard microzonation maps, using near-surface geotechnical and geophysical investigations, presenting their results as a series of maps, such as Vs, dominant alluvial period, and peak ground acceleration (PGA). Their conclusions have been simply relied on one-dimensional (1D) calculation transfer functions for soil profiles, considering the layers with the Vs of 700 m/s as the bedrock. In spite ofDespite this, the empirical studies reflecting on the site/reference spectral ratios on the earthquake data obtained from a temporary seismic network over the city have to date specified a significant difference, as compared with previous research, whether in terms of resonant frequency and amplification factor (Haghshenas, 2005). An example of the comparison between the analytical and empirical studies at one of the common stations in Tehran is presented in Table 1.

Table 1. Comparison of the results from seismic site effect analysis using analytical and empirical methods

Mofarah Hospital (KhaniAbadno Quarter)		Frequency (Hz)	Amplification
Analytical method	Jafari (2001), JICA (2000)	1.6-2.3	2-3
Empirical method	Haghshenas (2005)	0.5-0.7	>7

According to Haghshenas (2005), the existence of thick sedimentary layers with gradually increasing *Vs* and the basin edge effect are two probable reasons for such differences as well as the observation of low-resonance frequencies in Tehran. Such frequencies have been correspondingly reported and approved by other researchers (e.g., Shabani et al., 2011; Sohrabi Bidar et al., 2020).

The case of Tehran indicates that the rules that are normally applied in seismic regulations and codes, like the average *Vs* of surface layers down to 30 m (Vs30), and considering the layers with *Vs* higher than 650 m/s as seismic bedrocks (e.g., Building and Hous-

ing Research Center [BHRC], 2015; Building Seismic Safety Council [BSSC], 2020; International Code Council [ICC], 2018), as employed in Jafari (2001) and JICA (2000), fail to be a good choice for describing real site effects under such geological conditions.

This remarkable difference between the analytical and empirical results seems to be a matter of concern, as it is likely to cause an incorrect estimation of hazard parameters, and consequently lead to the improper design of buildings and infrastructure (Fazlavi & Asadian, 2021).

The safe design of urban structures, specifically the seismic response analysis of high-rise buildings, urban bridges, and other tall constructions with low natural frequency, accordingly requires a good evaluation of seismic site effects up to the proper depth of geological or seismic bedrocks (Che, Zhang, & Feng, 2016). Therefore, a critical step toward mitigating earthquake hazards in urban areas is to appropriately identify the characteristics of subsurface soil layers, especially the *Vs* structure, and its optimal modeling (Wycisk et al., 2009).

In the studies dealing with the seismic analysis of alluvial layers, the *Vs* profile is commonly determined using conventional experiments, such as drilling and surface geophysical methods, i.e., wave reflection and refraction as well as in-situ down-hole and cross-hole seismic surveying with active energy sources. In laboratory settings, cyclic tests are typically conducted on intact or reformed samples to determine shear modulus and *Vs*. Applying these conventional exploration techniques, wherein there are deep alluvial deposits, mainly in urban areas, is costly and even accompanied by the challenges of execution, such as the search for appropriate spaces for operations and the impossibility of the use of strong energy sources. In this sense, the utilization of some techniques based on passive energy sources, such as earthquakes and ambient noises (viz., microtremors), which are economical, repeatable, non-destructive, and easy to implement than conventional experiments is a suitable alternative in such fields (Shahsavani & Pirooz, 2009).

Exploiting ambient noises as single-station measurements (e.g., Bard, 1999; Ishida, Nozawa, & Niwa, 1998; Shankar et al., 2021; Chen et al., 2022) or the array ones (e.g., Horike, 1985; Matsushima & Okada, 1990; Fazlavi, 2014; Moghadasi & Shabani, 2022; Ahmadzadeh Irandoust, Priestley, & Sobouti, 2022) or single-station and array measurements together (e.g., Scherbaum, Hinzen, & Ohrnberger, 2003) have received much attention to determine the *Vs* profiles of the shallow and deep alluvial basins or estimate the velocity models of the Earth's upper crust, whose accuracy has also been proven (Kind, Fäh, & Giardini, 2005; Elbshbeshi et al., 2022). The basic assumptions of the methods developed on ambient noise measurements are that waves are stationary and wave fields are generally composed of surface waves. Ambient noise measurements have been similarly applied to investigate site effects in Tehran. A series of large-scale array measurements along two north-south and east-west sections of the city have been accordingly performed by Fazlavi (2014), in which the joint inversion of the Rayleigh wave dispersion curves, extracted by the spatial autocorrelation (SPAC) method, and the ellipticity curves of such waves, obtained by the horizontal-to-vertical time-frequency analysis (HV-TFA), had been used in order to illustrate deep *Vs* profiles in each measured site. As well, Shirzad and Hossein Shomali (2014) extracted the 1D *Vs* profiles of the Tehran sediments by cross-correlation based on long-time measurements (namely, five months of continuous data); however, the accuracy of the results, practically used for identifying deeper crust layers, could be under question for the depths less than 1 km (Fazlavi, 2014).

Against this background, the present study aims to extract the *Vs* structure of the subsurface layers in Hakimiyeh Valley in the eastern part of Tehran, considering no previous deep alluvial model of *Vs*, using the single-station and array measurements of ambient noise for assessing accurate site effects and finding the origin of the observed discrepancy between the previous analytical and empirical research outcomes. During this study, the efficiency of the single-station measurements in estimating the dynamic characteristics of alluvial layers in a valley basin is also evaluated.

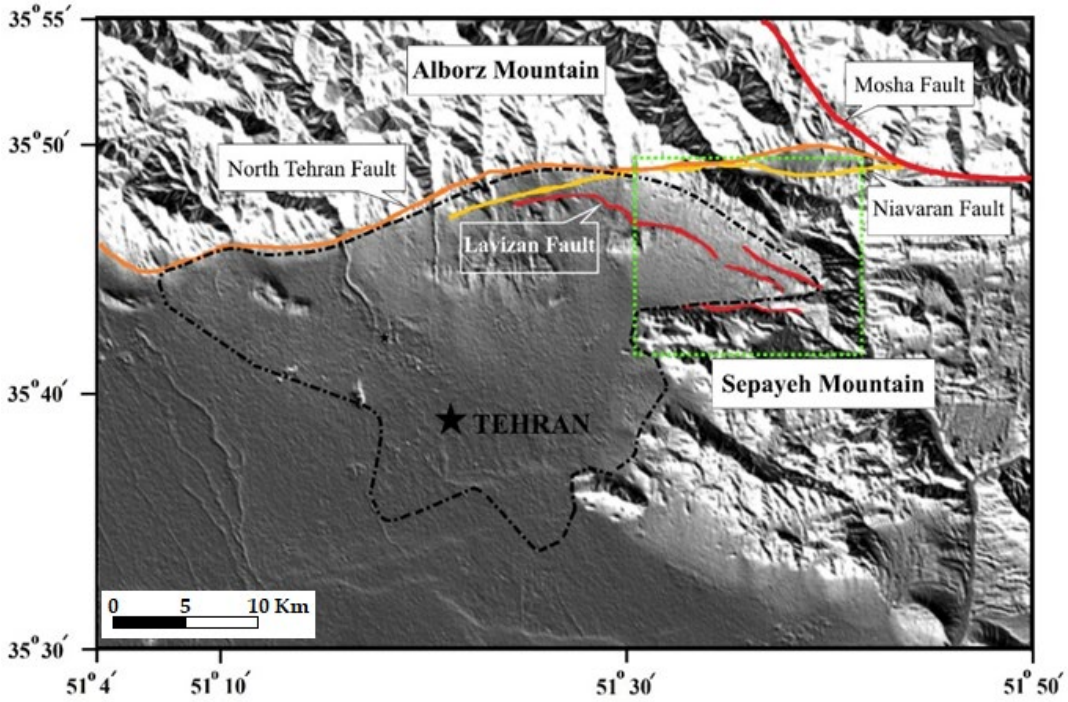

Figure 1. Hakimiyeh Valley borderlines (the green dotted line) and the critical faults passing through it (the red and orange continuous lines).

2 Study Area Geology

From the geological point of view, Hakimiyeh Valley is limited in the south to the Sepayeh mountains, with rock outcrops belonging to the Triassic, Jurassic, and Cretaceous periods, and then to the Alborz Mountain range on the northern side, mainly made up of the pyroclastic rocks of the Eocene-age Karaj Formation. From the east to the eastern Tehran hills, it further consists of the Pliocene-Quaternary coarse-grained alluviums (Geological Survey and Mineral Exploration of Iran [GSI], 1997). To the west, this valley joins the Tehran plain with a relatively mild topography, composed of the younger Quaternary alluviums (Rieben, 1955). This type of geomorphological setting accordingly means the existence of two-dimensional (2D) site effects in this area. On the other hand, the passage of quite a few faults through the basin may cause the formation of subsurface geometry due to the bedrock uplift or subsidence.

The urban area in Hakimiyeh Valley is mostly located over the coarse-grained alluvial deposits belonging to the young Quaternary ones (Pedrami, 1978). These sediments have originated from the rivers and seasonal floods initially poured from the Alborz mountains and its glaciers (Cheshmi, Fakher, & Khamehchian, 2008). Based on the classification presented by Rieben (1955), the Tehran alluviums have been divided into four series, A, B, C, and D, wherein Hakimiyeh Valley is predominantly filled with young alluvial fans of the C deposits.

The oldest and most powerful deposit in Tehran is a folded conglomerate formation named ‘A’ or HezarDareh. The ‘A’ Formation is deposited on the brittle bedrock of the piedmont and the southern limits are probably located at the end of the piedmont zone (Engalenc, 1968). In this respect, Rieben (1955) proposed the Pliocene-Early Pleistocene age for this formation, while Engalenc (1968) divided it into two Plio Quaternary and

Quaternary parts. Regarding lithology, this formation also consists of homogeneous conglomerates in which 85% of the pebbles are green tuffs from the Eocene-age Karaj Formation. According to Rieben (1955), the thickness of the 'A' deposits has a wide variety between 10 (close to the basin borders) and 1000 m (in the basin north-eastern part) with a decreasing thickness from the east to the west.

The subsequent formation, which unconformably overlays the 'A' Formation, is called the 'B' Formation, with a fluvioglacial origin coming from the north as well as deposits largely on the eroded surfaces of the 'A' Formation, resembling Alpine moraines. With respect to lithology, the 'B' Formation is composed of very heterogeneous materials from big boulders to grave grains, distributed in a silty matrix in the northern part of the city (Bn), while it consists of clay and sand materials in the south (Bs). The average thickness of the 'B' Formation is estimated to be 60%, but it strongly varies from place to place.

The 'C' Formation is also an alluvial conglomerate, covering most parts of the Tehran piedmont. The age of this formation is estimated from the middle to late Pleistocene. It further involves alluvial fans from the north to the south, with a moderate grain size wherein the proportion of coarser pebbles decreases from the north to the south. The average thickness for the 'C' Formation is estimated as 60 m (Rieben, 1955).

As well, the youngest stratigraphic part of the Tehran basin is the 'D' Formation, whose age is estimated to be less than 10000 years BP. With an alluvial and fluvial origin, the 'D' Formation comes from the northern mountain valleys and has deposits on the current or ancient riverbeds, spreading all over the Tehran plain to the south. The average thickness of the 'D' deposits, as observed in many boreholes, is 14 m.

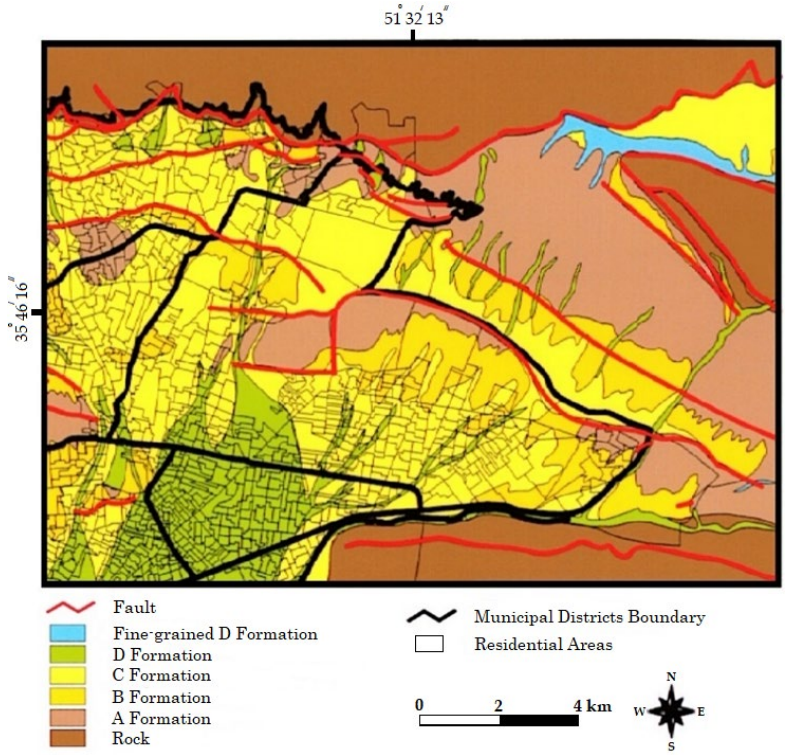

Figure 2. Distribution of the alluvial formations and rocks in Hakimiyeh Valley, filled with the young Quaternary alluvial deposits, consisting of A, B, C, and D formations (JICA, 2000).

3 Ambient Noise Measurement and Data Processing

In this study, the data are taken from a large project on the Tehran alluviums, which is currently being in progress by Haghshenas et al. in the International Institute of Earthquake Engineering and Seismology (IIEES). In order tTo extract the 2D velocity structure of Hakimiyeh Valley, the north-south and east-west profiles are considered along the ambient noise recorded data, and then processed by single-station and array measurement techniques.

As demonstrated in Figure 3, 11 single-station and 4 array measurements are used. In this respect, 4 locations including Shahid Abbaspour University of Technology (ABB), Iran University of Science and Technology (ELM), Third Square of Tehranpars (TSQ), and Police Park (PPK) are selected for the array measurements. Moreover, 11 seismic stations (Lennartz LE-3D/20s seismometers coupled with Parsian digitizers), arranged in two concentric circles, namely, 1 station in the center along with 3 and 7 stations respectively within the smaller and bigger circles are utilized in the array measurements.

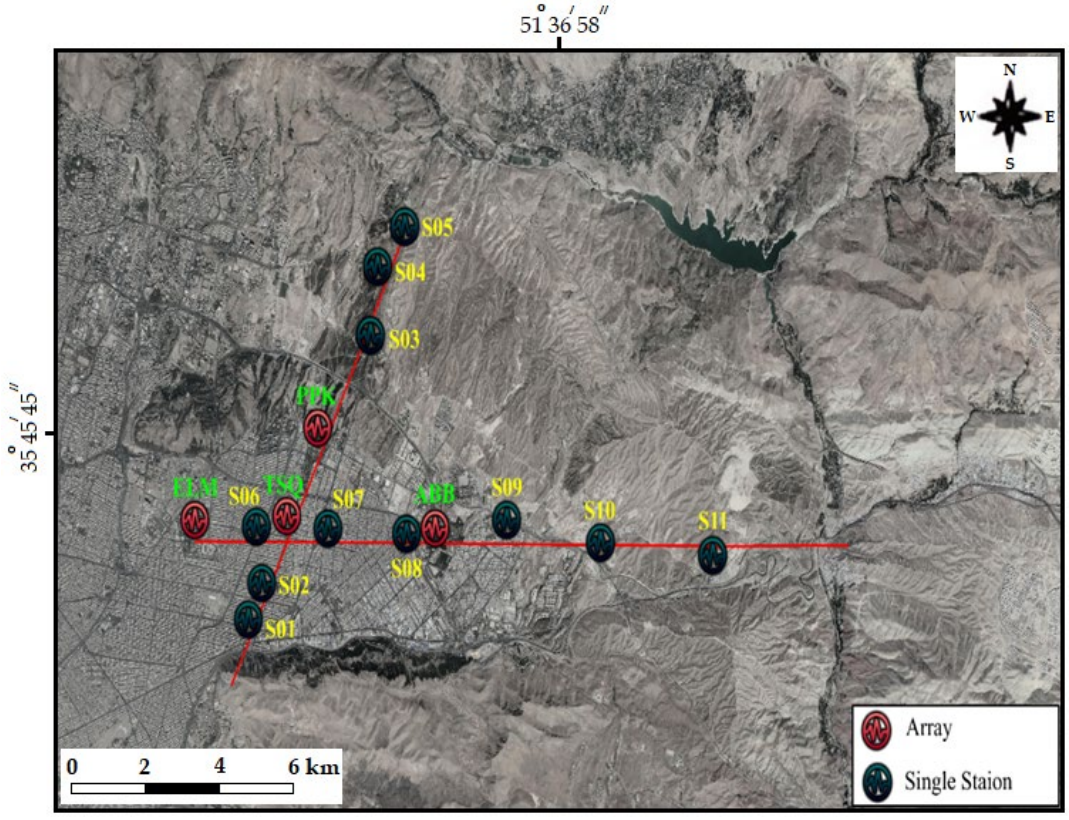

Figure 3. Location of the specified array and single stations for ambient noise measurement in Hakimiyeh Valley in this study.

The array layout is selected in such a way to allow for extracting the dispersion curves in the maximum range of frequency, considering the possibility of installation. In this regard, it is necessary to avoid the aliasing and resolution errors in the wavenumber space. The maximum and minimum wavenumbers (Kmax and Kmin) are thus selected, so that the value of the array transfer function (Eq. 1) always remains lower than 0.5 (Figure 5-a).

$$ATF(k) = \left| \frac{1}{M} \Sigma_{j=1}^{M} e^{i.\boldsymbol{r}_j.(\boldsymbol{k}_0 - \boldsymbol{k})} \right|^2 \qquad (1)$$

where M is the number of array stations, and (k_0-k) and r_j refer to the wavenumber and position vectors of the jth station, respectively. The reliable frequency range in the dispersion curve for a single array only depends on its layout. Therefore, determining the dimensions and layout of the stations in one array based on the above equations prevents the false increase in the power spectral density (PSD) within the frequency-wavenumber spaces and further misinterpretations (Schweitzer et al., 2012). The distances between the stations also control the searchable wavelengths. Tokimatsu (1997) has correspondingly proposed Eq. 2 to identify the valid boundaries of dispersion curves.

$$2D_{\min} < \lambda_{\min} < \lambda_{\max} < 3D_{\max} \qquad (2)$$

where D_min and D_max stand for the minimum and maximum distances between seismometers. As well, λ_min and λ_max represent the minimum and maximum wavelengths. The relationship between D_min and λ_min is further considered to prevent the aliasing error, and that between D_max and λ_max is assumed to put off the site filtering effects. Figure 4 demonstrates an example layout applied in the ELM array.

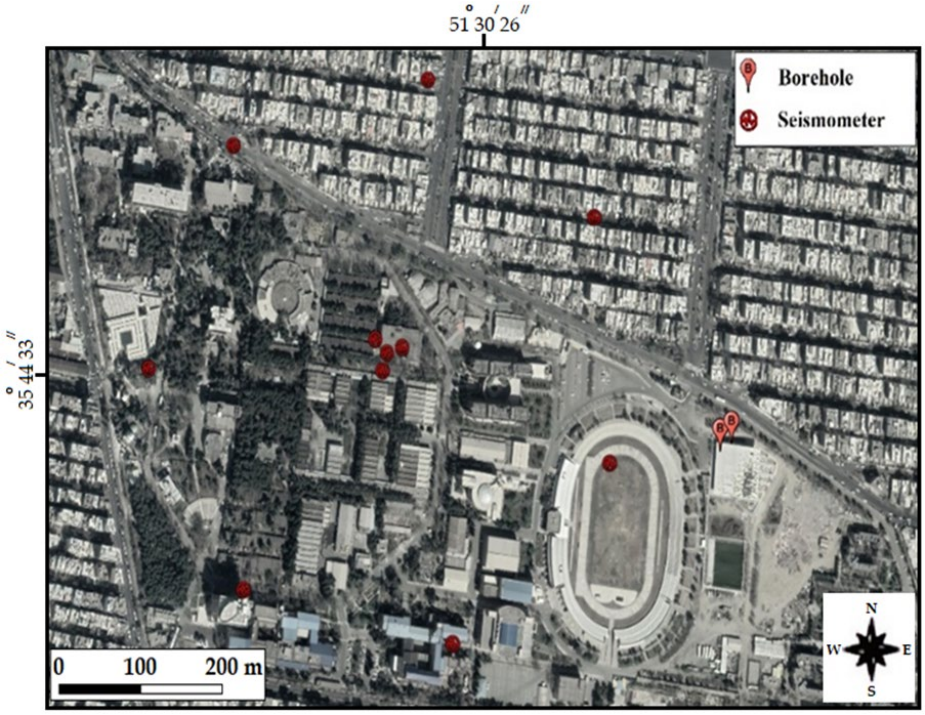

Figure 4. Seismometer layout and borehole location at the ELM station. A circular layout, including two concentric circles, is considered for the array measurements with 11 seismometers, 1 seismometer in the center, and 3 and 7 seismometers respectively within the smaller and bigger circles. The borehole data are utilized to extract the Vs of the surface layer.

Figure 5 indicates the array transfer function in the wavenumber space, and the values of Kmax=0.1713 and Kmin=0.0097 are obtained for the ELM station, wherein the reliable areas within the dispersion curve are specified by the red dashed line and the blue solid one, respectively. Eq. 1 and Figure 5-a show that the array layout can lead to a false increase in the seismic energy of all signals recorded by the array, and errors in the dispersion calculations of the Rayleigh waves out of the acceptable range (Figure 5-b).

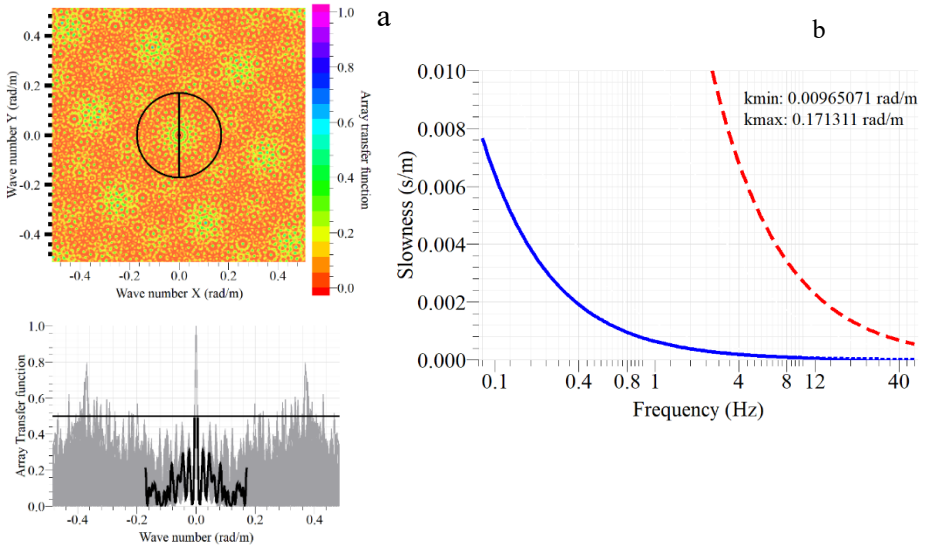

Figure 5. a) Array transfer function (Eq. 1) in the wavenumber space, and the maximum and minimum wavenumbers of the ELM array by assuming the maximum value of 0.5 for the transfer function calculated by the Geopsy software, and b) the allowable part of the dispersion curve in the frequency-slowness space between the upper (the red dashed line) and lower (the blue continuous line) limits.

The recording duration is 1 h for the arrays and 30 min for the single-station measurements. According to the requirements and rules presented in the Site Effects Assessment using Ambient Excitations (SESAME) project (Acerra et al., 2004); these durations could be enough for identifying the fundamental mode of the Rayleigh waves with frequencies higher than 0.2 Hz. In order tTo avoid the transient noises in the congested urban areas, such as TSQ, the array measurement is conducted between 3 and 4 am.

The data recorded by the array measurement are analyzed using the SPAC method and the frequency-wavenumber (F-K) analysis to extract the surface wave dispersion curves. Such curves are used in the inversion operation in conjunction with the Rayleigh wave ellipticity curve obtained from the HV-TFA of each station as well as other information, such as existing geotechnical and geophysical data, to reach the Vs profiles. In order tTo apply the array methods, the alluvial layers are assumed to be horizontal and parallel to each other, an even homogeneous. For the single-station data, inversion is further performed only using ellipticity curves and previous geophysical and geotechnical data. The 2D cross-sections of the alluvial basin in two directions, as shown in Figure 3, are further plotted by correlating the 1D profiles obtained from the mentioned inversion operation in each measured location.

3.1 SPAC

Aki (1957) defined the basis of the theory of the SPAC coefficient of determination and explained the method of estimating the surface wave phase velocity dispersion using the ambient noise recorded on a circular array of seismometers. Henstridge (1979) further developed a relationship between the SPAC coefficient and the fundamental mode of the Rayleigh waves. As well, Wathelet, Jongmans, and Ohrnberger (2005) presented the direct and immediate inversion of the SPAC coefficients as an alternative to the inversion of dispersion curves. Among numerous methods established to retrieve surface-wave phase velocities from ambient noise, SPAC has been thus one

of the most widely used techniques thanks to its robustness, ease of implementation, and computational efficiency (Hayashi et al., 2022). During SPAC, the coefficient curves are typically estimated by the power spectral density (PSD) resulting from the convolution of high-energy Rayleigh wave records of the microtremor, and the phase velocity is calculated via the zero-order Bessel function of the first kind (Fazlavi & Haghshenas, 2015). Since the array analyses are conducted on the Rayleigh waves, they are merely performed on the vertical component of the recorded seismograms, containing the Rayleigh wave information, to avoid disturbances from other surface waves, like the Love ones.

Given that there are some limitations in mounting seismometers on a perfect circular layout, the modified SPAC method proposed by Bettig et al. (2001) is applied in the present study. Accordingly, the SPAC coefficient for the nth ring, consisting of two circles of radius r_n1 and r_n2 with some seismometers on them is defined as follows:

$$\rho(\omega; r_{n1}, r_{n2}) = \frac{2}{r_{n2}^2 - r_{n1}^2} \int_{r_{n1}}^{r_{n2}} r\, J_0(kr)\, dr \qquad (3)$$

where k=k(ω) denotes the wavenumber, and J_0 (kr) refers to the zero-order Bessel function of the first kind. For this analysis, all pairs of stations are first specified. These stations with preserved azimuthal direction are then located, so that the azimuth is 0-180o and all pairs have the same origin. Now, regarding the distance of the stations from the center, some rings are defined, each one having some stations with almost equal distances. Figure 6 shows an example of the azimuthal arrangement of the seismometer pairs and the defined rings for TSQ.

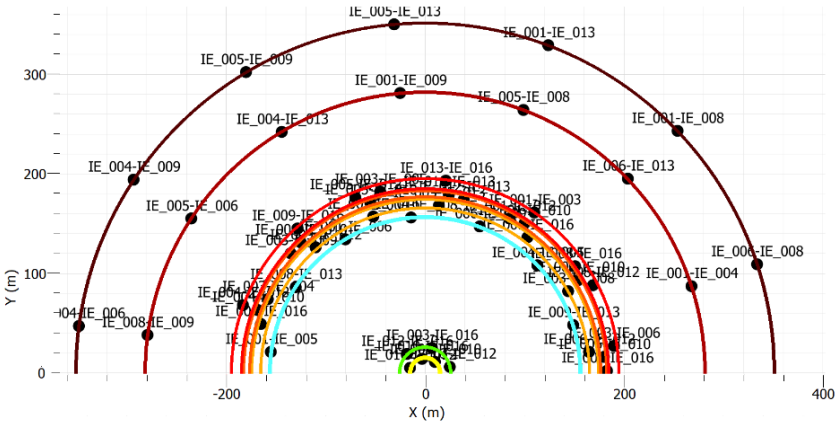

Figure 6. Representation of the seismometer pairs in the modified SPAC and the defined rings corresponding to their layouts in TSQ. According to the layout illustrated in Figure 4, all definable pairs of stations with preserved azimuthal direction are located with the same origin, so that the azimuth is between 0 and 180°.

In TSQ, 8 rings are defined concerning the layout of seismometers. Then, the autocorrelation and the corresponding dispersion curves are calculated for each ring by tapping SPAC. Regarding the Kmax and Kmin values and assuming the gradual increase in Vs with depth, the acceptable zone for each autocorrelation curve is filtered. Figure 7 exhibits the autocorrelation curves for the rings of array layout in TSQ.

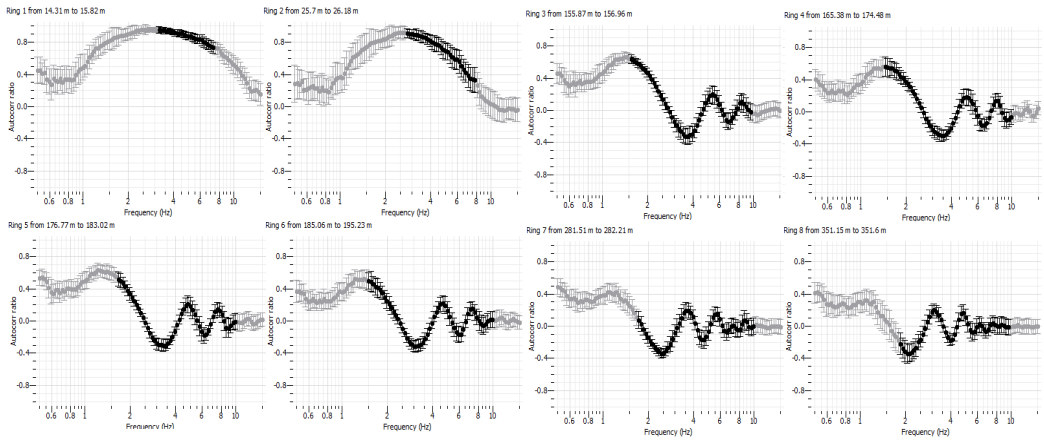

Figure 7. Autocorrelation curves for the defined rings of the array layout in TSQ. The acceptable zone is specified in black regarding the Kmax and Kmin values and the gradual increase in *Vs* with depth in the dispersion curve of each ring.

3.2. F-K Analysis

The F-K analysis is one other method for estimating the Vs of subsurface layers, introduced by Capon (1969) for the first time in the context of nuclear test detection. During the F-K analysis, it is assumed that waves pass through an array in a flat state with a zero angle (Lacoss, Kelly, & Toksöz, 1969). This method extracts phase velocity corresponding to the wavenumber vector and its frequency by deriving the correlation between vertical-component seismograms recorded at stations and PSD calculation (Fazlavi & Haghshenas, 2015). The F-K analysis output is the dispersion curve, demonstrating the relationship between phase velocity (or its inverse) and its corresponding frequency, which is applied as an objective function (OF) during the inversion operation. Figure 8 illustrates the refined dispersion curve obtained from the F-K analysis.

3.3 Ellipticity Analysis within Time-Frequency Domain

Although the Rayleigh wave is known as a surface one, it penetrates into the ground depth and provides useful information about the velocity structure in the subsurface layers of the site due to its elliptical motion and displacement of ambient particles concerning its wavelength. The ratio between the amplitude spectra of the horizontal-to-vertical components of the Rayleigh wave is named the ellipticity ratio, and regardless of the nature and cause of formation, the ellipticity of the Rayleigh waves at the resonant frequency of the site shows a clear peak (Fäh, Kind, & Giardini, 2001).

Figure 8. a) Dispersion curve at PPK station resulting from the F-K analysis, b) Filtered curve in the allowable region of dispersion curve based on Kmax and Kmin calculated from Eq. 1. Despite the presence of a wider acceptable range of wavenumbers, a smaller region is selected due to improper correlation for frequencies over 5.5 Hz.

Ellipticity is one of the properties of the Rayleigh waves, which has received much attention in site effect studies over recent decades, and researchers have investigated different methods to extract ellipticity using single-station measurements. In the Joint Research Activity 4 (JRA4) report of the Network of Research Infrastructures for European Seismology (NERIES), the TFA based on the Morlet wavelet transform of horizontal and vertical-component spectra of signals or ambient noises is introduced, and its spectral ratio curves are plotted with some operational examples at multiple European sites (Fäh et al., 2010). By examining the ellipticity

curves of various sites, it is observed that the right flank of the spectral ratio curve, namely, the section between the peak and the first trough after it, corresponds well with the ellipticity curves of the Rayleigh waves for a given ground model (Hobiger et al., 2013). This right flank of the HV-TFA curve, as well as the peak, can be thus utilized as two OFs in the inversion operation to extract the ground velocity model.

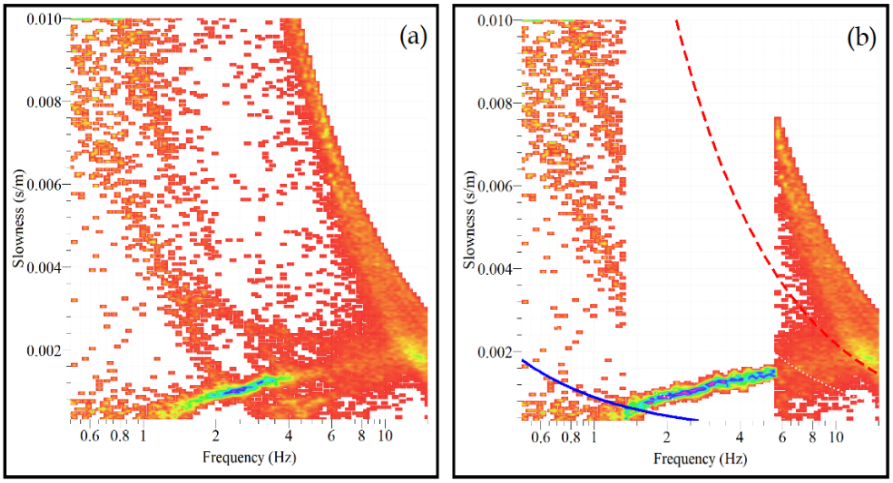

Figure 8. a) Dispersion curve at PPK station resulting from the F-K analysis, b) Filtered curve in the allowable region of dispersion curve based on Kmax and Kmin calculated from Eq. 1. Despite the presence of a wider acceptable range of wavenumbers, a smaller region is selected due to improper correlation for frequencies over 5.5 Hz.

In this study, the TFA is performed for all array and single-station measurements. With regard toConcerning the array measurement, only the average ellipticity curve of all stations is considered. Figure 9 shows an example of the average ellipticity curve calculated by the HV-TFA at 11 stations in the TSQ array.

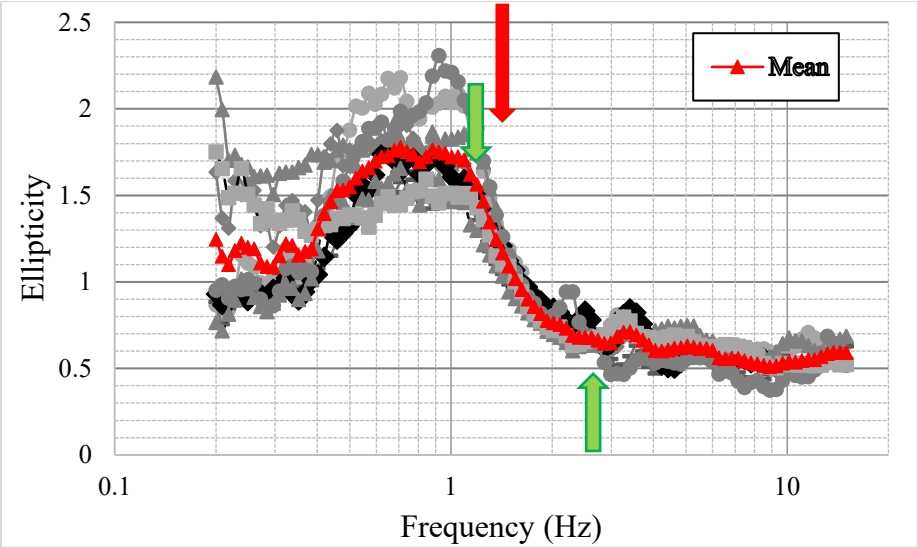

Figure 9. Ellipticity curves resulting from the TFA of the TSQ station array measurement and the average of ellipticity curves. The right flank of ellipticity is specified by green arrows, and the dominant frequency is illustrated by a red arrow.

3.4 Inversion and Vs Profile Extraction

The penetration depth of the Rayleigh waves in ground layers depends on the vibration frequency and its dispersive property that is controlled by the Vs structure of the environment. This allows for finding the Vs profile of the ground layer, through the inversion of dispersion and the ellipticity curves of the Rayleigh waves. In a general definition, the inversion of the surface waves defines the process of realizing the best-layered earth models, whose theoretical dispersion curves have the lowest misfit/error (Eq. 4), as compared with the empirical data (Wathelet et al., 2005).

$$misfit = \sqrt{\frac{1}{n}\sum_{i=1}^{n}\frac{(c_{di}-c_{ci})^2}{\sigma_i^2}} \quad (4)$$

where c_di represents the observed data values, c_ci is the average of the calculated data, σ_i stands for the variance of the data at the frequency f_i , and n shows the number of frequency intervals.

The neighborhood algorithm (Sambridge, 1999a, 1999b; Wathelet, 2008), as one of the most used global search ones for surface wave inversion, is further applied in this study for the inversion of the OFs and the extraction of the Vs profiles.

In this vein, Wathelet (2005) exploited the neighborhood algorithm to determine the Vs profiles, using the direct inversion of the SPAC coefficient and the dispersion curves of the surface waves, and enhanced the algorithm efficiency by improving the selection of parameters. The misfit value (Eq. 4) of the theoretically calculated dispersion or ellipticity curves with each empirically obtained OF is thus individually calculated to determine the weighted average misfit values. By directing the models toward the misfit value minimization in several runs of inversion, the best Vs profile is estimated for each measured site. The neighborhood algorithm flowchart is presented in Figure 10.

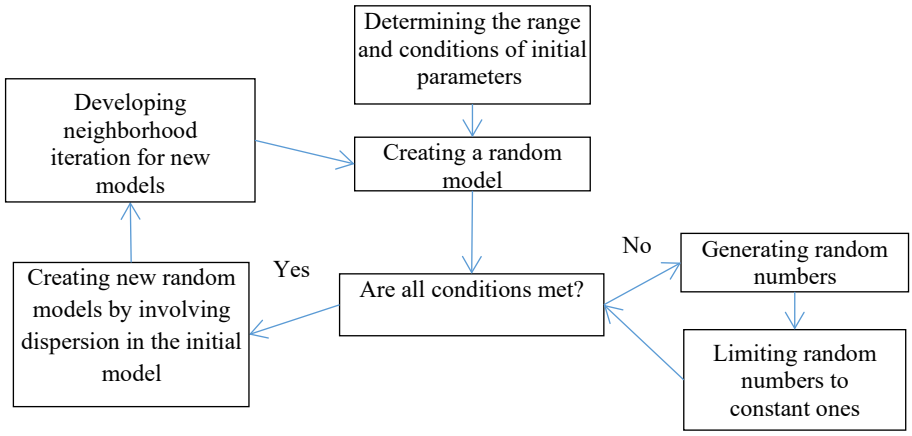

Figure 10. Neighborhood algorithm flowchart (Fazlavi, 2014).

In order tTo extract the Vs profile at the array stations, the joint inversion of the auto-correlation ratio curves and the Rayleigh wave dispersion ones, with the right flank of the ellipticity curve and the site dominant frequency, are exploited as depicted in Figure11. To extract the Vs profile at the single stations, only the right flank of the ellipticity curve and the site dominant frequency are recruited. For making the input model of the inversion operation, the conditions of the surface layers are further estimated for each single-station or array measurement site, concerning the logs of the drilled boreholes around the stations, experiment outcomes, or the seismic classification of the site bedrock, according to the

National Earthquake Hazards Reduction Program (NEHRP) regulations (Shafiee & Azadi, 2007). One of the economical and uncomplicated methods of estimating the Vs of surface layers is also the standard penetration test (SPT) (Abbasi, 2011). At the stations where the information about the geotechnical boreholes is available, the Vs of the layers is accordingly extracted using the SPT results and the empirical correlations,proposed by Athanasopoulos (1970). The Vs of the surface layers is thus used as the boundary conditions of these layers during the inversion operation. Regarding the previous knowledge about the characteristics of the Tehran alluviums that shows a gradual increase in the Vs with depth, the input model layer parameterization is individually and uniformly performed for each layer with a growing trend relative to the previous one. The input models utilized in the inversion operation for the array measurement are demonstrated in Table 2.

At all sites under investigation here, adequate geotechnical and geophysical information is available for the shallow depths less than 30 m. Accordingly, two or three layers with uniform velocities are defined. For the layers deeper than 30 m, 5 to 7 uniform layers without any limitations in their velocity or thickness are also considered on the hard bedrock, depending on the dominant frequency of the site. Density is further assumed to be between 2000 and 2200 kg/m3, and the Poisson's ratio in the range of 0.15-0.4 is used in the inversion operation. Figure 12 displays the inversion results for the ELM array. The inversion uncertainty is much more in the single-station measurement, as compared with the array data; however, there is an attempt to reduce it using other available geological-geophysical data. For example, the results are compared with those of the arrays implemented near the single-station measurement, and the profiles with significant differences within the array data are rejected.

Table 2. Initial parametrization of the layers during the inversion operation for the array measurement stations.

Number of layers	Depth	ELM	TSQ	PPK	ABB
	(m)	Vs ($m.s^{-1}$)			
2-3 layers in geotechnical data	0-5	300-450	300-400	300-450	300-420
	5-10	450-600	400-500	450-3600	500-550
	10-30				700-750
7 layers to converge the best model	30-100	600-3600	500-3600	450-3600	750-3600
	30-200	600-3600	500-3600	450-3600	750-3600
	30-400	600-3600	500-3600	450-3600	750-3600
	30-800	600-3600	500-3600	450-3600	750-3600
	30-1200	600-4500	500-4500	450-4500	750-4500
	30-1600	600-4500	500-4500	450-4500	750-6000
	30-2000	600-4500	500-4500	450-4500	750-6000
1 layer	Bedrock	1500-6000			

4 Results and Conclusion

The 2D *Vs* profiles of the study area are made by the integration and interpolation of the 1D ones at each measured site. An example of the data tapped during the inversion operation and the 1D profile extraction is illustrated in Figure 12 for the ELM site. The final profiles are further selected among those with the lowest misfit (in red, Figure 12a). Two criteria are further employed in the selection of the final velocity profile among all desirable models with the lowest misfit. The first one is the $\frac{V_p}{V_s}$ ratio. Since it is directly correlated with the porosity of the alluvial layers (Lee, 2002), the logic range for $\frac{V_p}{V_s}$ is 1.8-2.3, based on the geological information about the alluvial deposits of Hakimiyeh Valley, so the profiles that satisfy these ratios are selected. The second criterion is the similarity (in shape and amplitude) between the ellipticity curves obtained and the HV-TFA curve observed, not only at the right flank but also in the entire frequency range up to the end of the curves. The 1D *Vs* profiles for all measured sites are presented in Figure 13.

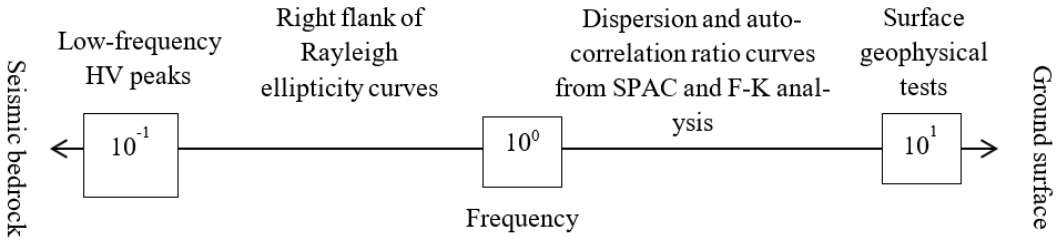

Figure 11. Diagram of the frequency range of empirical OFs in the inversion operation for determining the *Vs* profile in the Tehran area (Fazlavi & Haghshenas, 2015). In the Hakimiyeh Valley alluvial basin, the majority of low-frequency HV peaks vary from 0.5 up to 1.5 Hz, the right flank of the Rayleigh ellipticity fluctuates from the HV peaks up to 3 Hz, and the dispersion and autocorrelation ratio curves vary from 2 Hz up to 8 Hz.

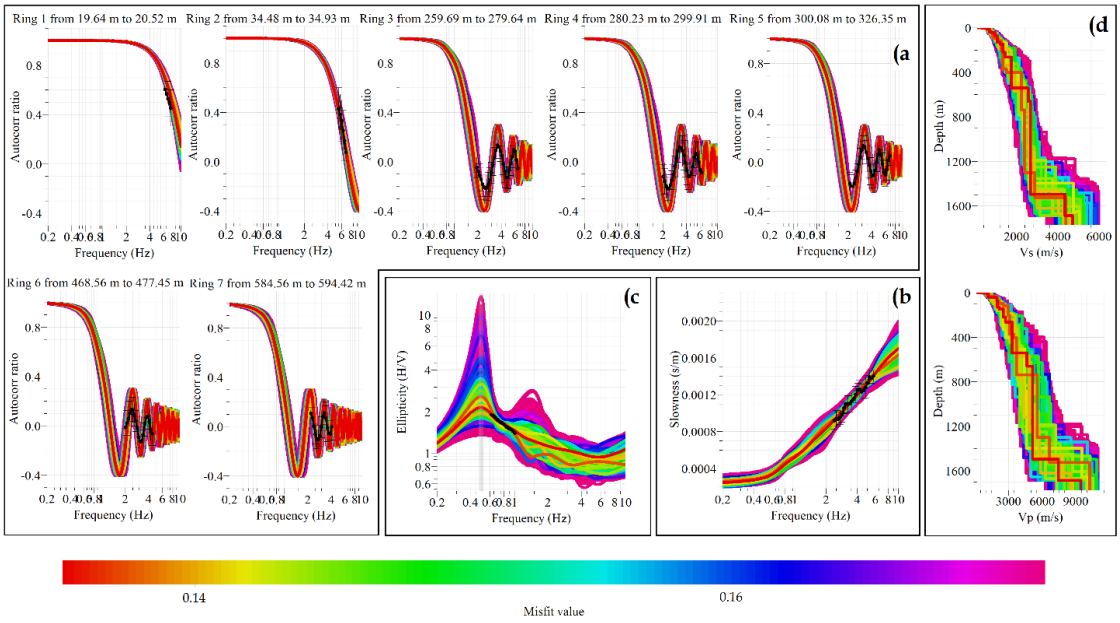

Figure 12. Conformance of the theoretical curves of the inverted *Vs* profiles (colorful curves) with empirical OFs (black curves), including (a) auto-correlation ratio curves, (b) Rayleigh wave dispersion curve, and (c) right flank of ellipticity curve with site dominant frequency. (d) Theoretical shear-wave and pressure-wave velocity profiles obtained from the inversion of OFs at the ELM array station. According to the colorful contour of the misfit, the red inverted curves have the minimum misfit, and the purple ones have the maximum misf.

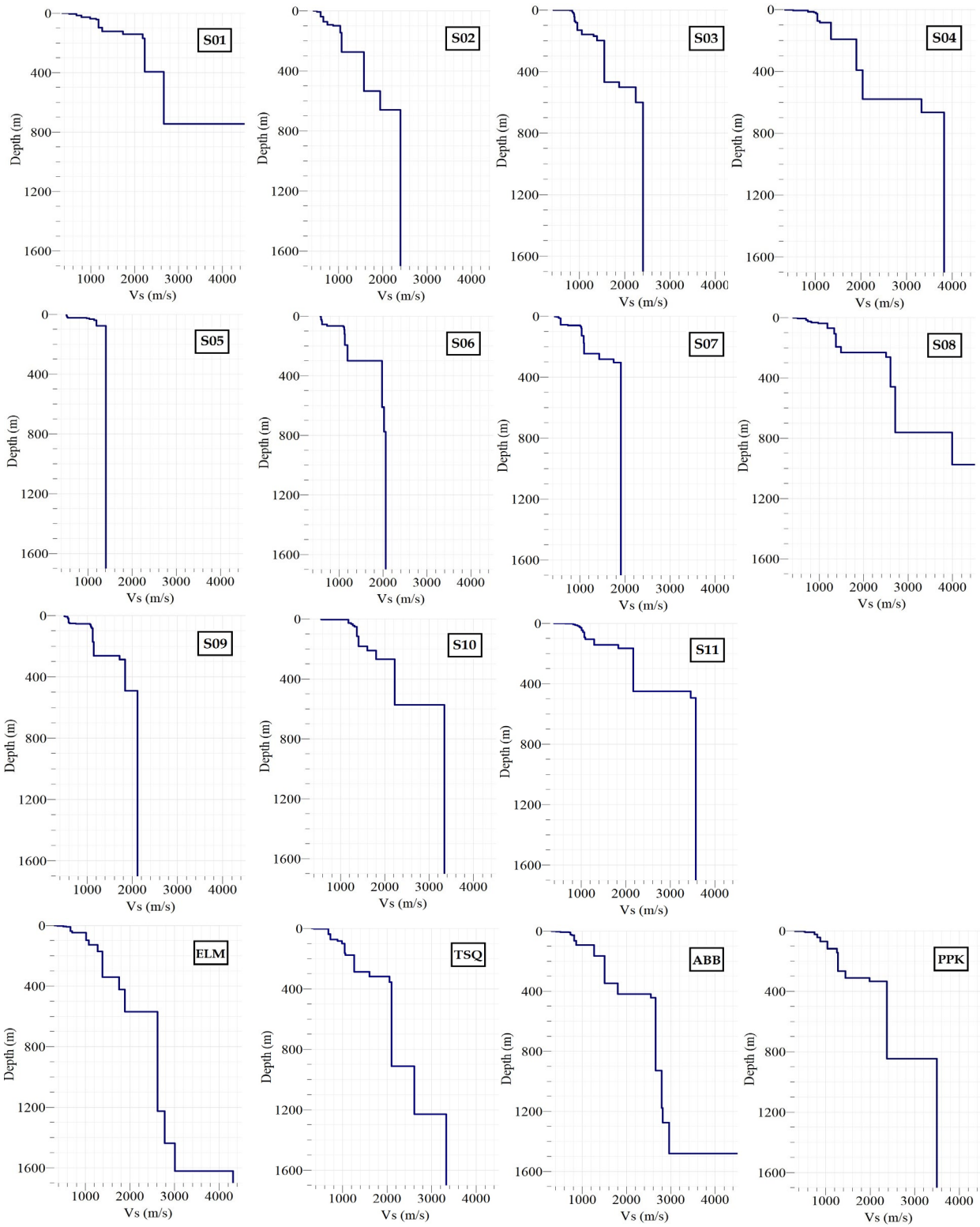

Figure 13. Selected 1D *Vs* profiles at all measurement stations of the ambient noises, estimated using the inversion operation of the empirical OFs.

Now, the 2D Vs models are derived by interpolating the 1D profiles with the specified velocity ranges as shown in Figure 14 and Figure 15. These 2D models of Hakimiyeh Valley are thus the first deep ones in this alluvial basin.

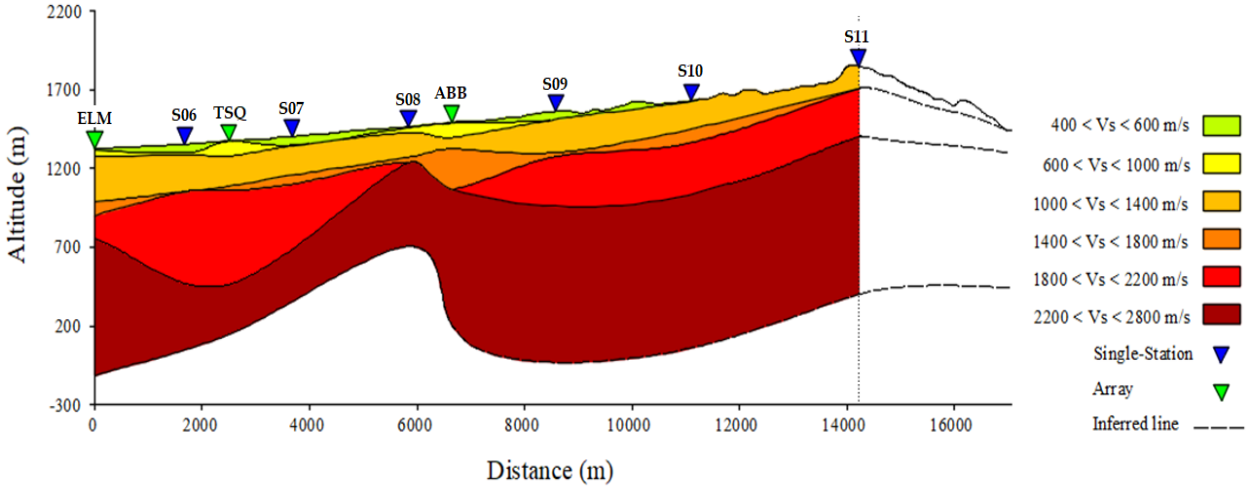

Figure 14. 2-D east-west *Vs* profile in Hakimiyeh Valley estimated by interpolating the 1D *Vs* profiles.

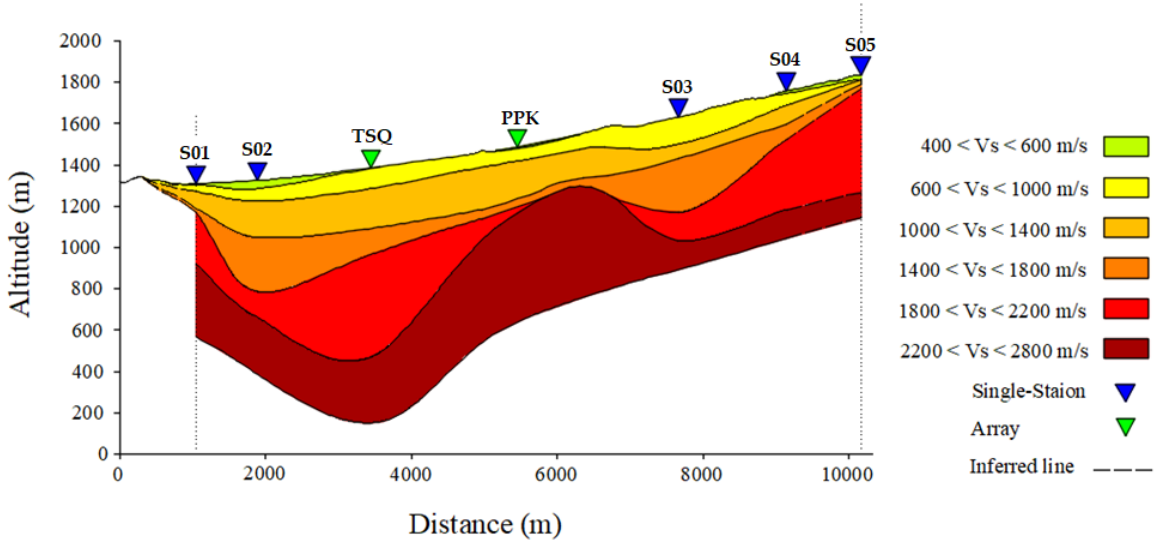

Figure 15. 2-D north-south *Vs* profile in Hakimiyeh Valley estimated by interpolating the 1D *Vs* profiles.

As illustrated in Figure 13, the main velocity contrast of the 1D profiles occurs in the range of 2000 to 2200 m/s, which corresponds to the dominant frequency of the site. Although the velocities higher than 2200 m/s are observed in the figures, the results for those higher than 2200 or the related contrast values are not reliable due to the lack of observational data or empirical OFs. For instance, the velocity value after the last contrast at the ELM station is not interpretable, but there is a hard layer under it. Upon comparing the results with previous geo-seismic surveys on the rock outcrops at the edge of the sedimentary basin, as presented in Table 3, it seems that the velocity of 2200 m/s and higher matches the geological bedrock of the basin, whose depth in the deepest part of the alluvial basin reaches over 800 m. The Vs of the bedrock and its depth are is also completely different from those in previous analytical studies, which lead to big mistakes in predicting seismic hazards and designing safe structures, especially in the case of high-rise buildings.

Table 3. Measured *Vs* at the rock outcrops of the northern, eastern, and southern parts of Tehran (Shafiee & Azadi, 2007).

Site classification	Vs (30) (m/s)	Type of materials	Zone
A	1600	Dolomite	Eastern and southern mountains
B	1400	Limestone	
B	1200	Marly limestone	
A	2500	Basalts	Northern mountains
A	2000	Andesites and pyroclastics	
B	1300	Shales and tuffs	

The analytical dominant frequency of the sediments in Hakimiyeh Valley, presented in JICA (2000) and Jafari (2001), have some discrepancies with that extracted from the measurement of the ambient noises and the 1D profiles in the present study. As depicted in Figure 16, no sharp and clear peaks can be observed in the analytical amplification functions in Hakimiyeh Valley, while there are distinct peaks in the range below 2 Hz for all stations in the present study, except for S05, which should be considered in future analytical investigations. As shown in Figure16, the maximum depth for the bedrock is 20 m, while it is much deeper in the present study

Evidence represents that the velocity structure estimated by measuring ambient noises properly indicates the variations of geological layers (Ehsani et al., 2015), but generally, such models can be employed for the dynamic analysis of site effects, as they are derived from empirical OFs.

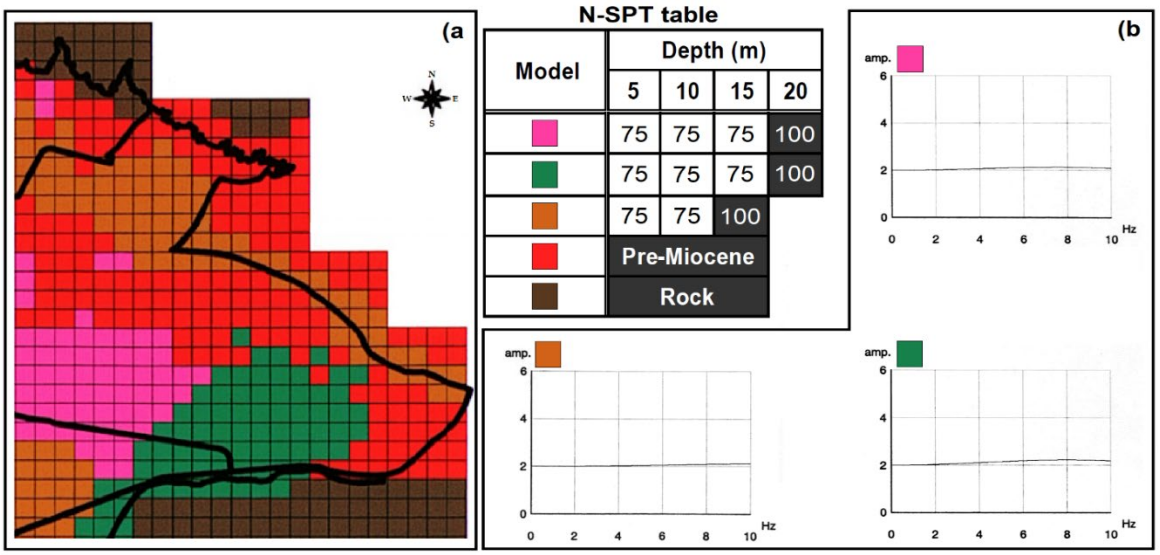

Figure 16. (a) Microzonation of the ground models and the geological logs in Hakimiyeh Valley. The pink and brown models are filled with gravel, and the green model is formed with sand. (b) Amplification function in the frequency domain based on the specified logs (JICA, 2000).

In the north-south profile, the changes in the seismic bedrock show the obvious folding caused by the Lavizan fault. Besides, a similar folding can be seen in the east-west profile, related to the Lavizan fault located along it and buried

under the sediments in this part, according to the geological conditions of the region. The Lavizan normal fault, which has created the outcrop of the Hezardareh or 'A' Formation, has been further eroded over times, and has ultimately filled Hakimiyeh Valley and the Tehran plain.

The 2-D Vs structure with two different orientations in Hakimiyeh Valley implies that the variations in the velocity and dynamic properties of the soil in this area, as one with a complicated subsurface structure, are significant. However, definitive judgment about this issue requires more thorough studies and the presentation of a 3D model of the velocity structure of this area. The study area with more array and single-station measurements is thus to be considered in the coming months in order to extract a full 3D model of Vs. The 3D numerical simulation of the model under synthetic earthquakes is also one part of the future work. As well, there is an attempt to confirm the findings about the bedrock depth and underground topography of this alluvial basin. At last, the following question is to be addressed: What are the impacts of the 3D geometry of Hakimiyeh Valley on seism

References

BSSC (Building Seismic Safety Council) (2020). NEHRP Recommended Provisions for Seismic Regulations for New Buildings and Other Structures, Part1 Provisions. National Institute of Building Sciences.

GSI (Geological Survey and Mineral Exploration of Iran) (1997). Geological map of Iran, Sheet No. 6361. Tehran, Iran.

ICC (International Code Council) (2018). 2018 International Building Code. ICC Retrieved from https://codes.iccsafe.org/content/IBC2018

Abbasi, M. (2011). The relationship between shear wave velocity and the number of standard penetration test in Mashhad alluvium, The 6th National Civil Engineering Congress, Semnan, Iran https://civilica.com/doc/120507

Acerra, C., Aguacil, G., Anastasiadis, A., Atakan, K., Azzara, R., Bard, P.-Y., Basili, R., Bertrand, E., Bettig, B., & Blarel, F. (2004). Guidelines for the implementation of the H/V spectral ratio technique on ambient vibrations measurements, processing and interpretation. No. European Commission–EVG1-CT-2000-00026 SESAME. Brussels, Belgium: European Commission.

Ahmadzadeh Irandoust, M., Priestley, K., & Sobouti, F. (2022). A Seismic investigation of the upper crustal structure of the Iranian plateau. Iranian Journal of Geophysics, 15(4), 115-126.

Aki, K. (1957). Space and time spectra of stationary stochastic waves, with special reference to microtremors. Bulletin of the Earthquake Research Institute, 35, 415-456.

Athanasopoulos, G. (1970). Empirical correlations Vso-NSPT for soils of Greece: A comparative study of reliability. WIT Transactions on The Built Environment, 15.

Bard, P.-Y. (1999). Microtremor measurements: a tool for site effect estimation. In Proc. of 2nd Int. Symp. on the Effects of Surface Geology on Seismic Motion.

Bettig, B., Bard, P., Scherbaum, F., Riepl, J., Cotton, F., Cornou, C., & Hatzfeld, D. (2001). Analysis of dense array noise measurements using the modified spatial auto-correlation method (SPAC): application to the Grenoble area. Bollettino di Geofisica Teorica ed Applicata, 42(3-4), 281-304.

BHRC (Building and Housing Research Center) (2015). Iranian code of

practice for seismic resistant design of buildings (4th edition). Road, Housing & Urban Development Research Center Tehran, Iran. (In Persian)

Capon, J. (1969). High-resolution frequency-wavenumber spectrum analysis. Proceedings of the IEEE, 57(8), 1408-1418.

Che, A.-l., Zhang, T.-y., & Feng, S.-k. (2016). Characteristics of long period microtremor and validation of microtremor array measurements in inland areas of China. Journal of Mountain Science, 13(11), 1910-1922.

Cheshmi, A., Fakher, A., & Khamehchian, M.A. (2008). Geology of Tehran Alluvium and Evaluation of Rieben Classification for Geotechnical Studies. Journal of Science (University of Tehran) (JSUT), 34(2), 1-15. SID. https://sid.ir/paper/2208/en (In Persian)

Chen, C. T., Kuo, C. H., Lin, C. M., Huang, J. Y., & Wen, K. L. (2022). Investigation of shallow S-wave velocity structure and site response parameters in Taiwan by using high-density microtremor measurements. Engineering Geology, 297, 106498.

Ehsani, N., Ghaemghamian, M. R., Fazlavi, M., & Haghshenas, E. (2015). Estimation of subsurface structure using microtremor in Karaj city, Iran. 10th Asian Regional Conference of IAEG,

Elbshbeshi, A., Gomaa, A., Mohamed, A., Othman, A., & Ghazala, H. (2022). Seismic hazard evaluation by employing microtremor measurements for Abu Simbel area, Aswan, Egypt. Journal of African Earth Sciences, 196, 104734.

Engalenc, M. (1968). Contribution a la Geologie, Geomorphologie, Hydrogeologie de la region de Tehran (Iran). CERH, Montpellier, France, 365.

Fäh, D., Kind, F., & Giardini, D. (2001). A theoretical investigation of average H/V ratios. Geophysical Journal International, 145(2), 535-549.

Fäh, D., Poggi, V., Marano, S., Michel, C., Burjanek, J., Bard, P., Cornou, C., Wathelet, M., Renalier, F., & Hobiger, M. (2010). Guidelines for the implementation of ambient vibration array techniques: measurement, processing and interpretation. NERIES deliverable JRA4-D9.

Fazlavi, M. (2014). Investigation of Seismic Properties of Deep Alluvium by Array Analysis of Environmental Vibrations (Case Study in Tehran) [Doctoral dissertation, International Institute of Earthquake Engineering and Seismology (IIEES)]. (In Persian)

Fazlavi, M., & Asadian, A. (2021). Evaluation of Changing Effects of Density and Thickness of Polyurethane as a Protective Coating on Underground Tunnels under Surface Blast. Karafan Quarterly Scientific Journal, 18(1), 119-134.

Fazlavi, M., & Haghshenas, E. (2015). Importance of mode detection in ambient noise array application for shear wave velocity profile determination. International Journal of Civil Engineering, 13(1), 62-72.

Foutch, D. A., Hjelmstad, K. D., Calderón, E. D. V., Gutiérrez, E. F., & Downs, R. E. (1989). The Mexico earthquake of September 19, 1985—Case studies of seismic strengthening for two buildings in Mexico City. Earthquake Spectra, 5(1), 153-174.

Haghshenas, E. (2005). Geotechnical Conditions and Local Seismic Hazards in Tehran [Doctoral dissertation, Joseph Fourier University-Grenoble I]. (In French)

Hayashi, K., Asten, M. W., Stephenson, W. J., Cornou, C., Hobiger, M., Pilz, M., & Yamanaka, H. (2022). Microtremor array method using spatial autocorrelation analysis of Rayleigh-wave data. Journal of Seismology, 26(4), 601-627.

Henstridge, J. D. (1979). A signal processing method for circular arrays. Geophysics, 44(2), 179-184.

Hobiger, M., Cornou, C., Wathelet, M., Giulio, G. D., Knapmeyer-Endrun, B., Renalier, F., Bard, P.-Y., Savvaidis, A., Hailemikael, S., & Le, B. N. (2013). Ground structure imaging by inversions of Rayleigh wave ellipticity: sensitivity analysis and application to European strong-motion sites. Geophysical Journal International, 192(1), 207-229.

Horike, M. (1985). Inversion of phase velocity of long-period microtremors to the S-wave-velocity structure down to the basement in urbanized areas. Journal of Physics of the Earth, 33(2), 59-96.

Ishida, H., Nozawa, T. and Niwa, M. (1998). Estimation of deep structure based on phase velocities and spectral ratios of long-period microtremors. In Proc. of 2nd Int. Symp. on the Effects of Surface Geology on Seismic Motion.

Jafari, M. K. (2001). Complementary Microzonation Studies for South of Tehran. Research report no. 5017. International Institute of Earthquake Engineering and Seismology (IIEES).(In Persian)

Jafari, M. K. (2001). Site Effect Microzonation for North of Tehran. Research report no. 5018. International Institute of Earthquake Engineering and Seismology (IIEES). (In Persian)

JICA (Japan International Cooperation Agency) (2000). The study on seismic microzoning of the Greater Tehran Area in the Islamic Republic of Iran. Pacific Consultants International Report, OYO Cooperation, Japan, 291-390.

Kind, F., Fäh, D., & Giardini, D. (2005). Array measurements of S-wave velocities from ambient vibrations. Geophysical Journal International, 160(1), 114-126.

Lacoss, R. T., Kelly, E. J., & Toksöz, M. N. (1969). Estimation of seismic noise structure using arrays. Geophysics, 34(1), 21-38.

Lee, M. W. (2002). Biot–Gassmann theory for velocities of gas hydrate-bearing sediments. Geophysics, 67(6), 1711-1719.

Matsushima, T., & Okada, H. (1990). Determination of deep geological structures under urban areas using long-period microtremors. Butsuri Tanko (Geophysical Exploration); (Japan), 43(1).

Moghadasi, N. S., & Shabani, E. (2022). Impact of distribution of seismic ambient noise sources on surface wave characteristics. Iranian Journal of Geophysics, 15(4), 1-14.

Pedrami, M. (1978). Brief information about Quaternary sediments around Tehran. https://www.gsi.ir/Images/engeo/quaternary.pdf (in Persian)

Rieben, H. (1955). The geology of the Teheran plain. American Journal of Science, 253(11), 617-639.

Sambridge, M. (1999). Geophysical inversion with a neighbourhood algorithm—I. Searching a parameter space. Geophysical journal international, 138(2), 479-494.

Sambridge, M. (1999). Geophysical inversion with a neighbourhood algorithm—II. Appraising the ensemble. Geophysical Journal International, 138(3), 727-746.

Scherbaum, F., Hinzen, K. G., & Ohrnberger, M. (2003). Determination of shallow shear wave velocity profiles in the Cologne, Germany area using ambient vibrations. Geophysical Journal International, 152(3), 597-612.

Schweitzer, J., Fyen, J., Mykkeltveit, S., Gibbons, S. J., Pirli, M., Kühn, D., & Kværna, T. (2012). Seismic arrays. In New manual of seismological

observatory practice 2 (NMSOP-2) (pp. 1-80). Deutsches GeoForschungsZentrum GFZ.

Shabani, E., Mirzaei, N., Haghshenas, E., & Eskandari-Ghadi, M. (2011). A revised spatial autocorrelation method to study shear wave velocity. Journal of the Earth and Space Physics, 37(3), 71-85.

Shafiee, A., & Azadi, A. (2007). Shear-wave velocity characteristics of geological units throughout Tehran City, Iran. Journal of Asian Earth Sciences, 29(1), 105-115.

Shahsavani, H. & Pirooz, I. (2009). Comparison of shear wave velocity profile of subsurface layers obtained by DHT method with SASW and MASW methods: a case study in Shahrood University of Technology. The 8th International Congress of Civil Engineering, Shiraz, Iran. https://civilica.com/doc/62561 (In Persian)

Shankar, U., Kumari, S., Yadav, P. K., Singh, A. P., & Gupta, A. K. (2021). Microtremor measurements in the India's holy city, Varanasi for assessment of site characteristics. Quaternary International, 585, 143-151.

Shirzad, T., & Hossein Shomali, Z. (2014). Shallow crustal structures of the Tehran basin in Iran resolved by ambient noise tomography. Geophysical Journal International, 196(2), 1162-1176.

Sohrabi Bidar, A., Maghami, Sh., Zarean, A. & Asghari Koljahi, E. (2020). Investigating the convergence of shear wave velocity structure models resulting from the analysis of ellipticity curves of surface waves of ambient noises 1. Journal of Engineering Geology, 13(4), 15-27. SID. https://sid.ir/paper/958603/fa (In Persian)

Tokimatsu, K. (1997). Geotechnical site characterization using surface waves. Earthquake geotechnical engineering.

Wathelet, M. (2005). Array recordings of ambient vibrations: surface-wave inversion [PhD Diss., Liége University].

Wathelet, M. (2008). An improved neighborhood algorithm: parameter conditions and dynamic scaling. Geophysical Research Letters, 35(9).

Wathelet, M., Jongmans, D., & Ohrnberger, M. (2005). Direct inversion of spatial autocorrelation curves with the neighborhood algorithm. Bulletin of the Seismological Society of America, 95(5), 1787-1800.

Wycisk, P., Hubert, T., Gossel, W., & Neumann, C. (2009). High-resolution 3D spatial modelling of complex geological structures for an environmental risk assessment of abundant mining and industrial megasites. Computers & Geosciences, 35(1), 165-182.